Bovine bone matrix/poly(L-lactic-*co*-ε-caprolactone)/gelatin hybrid scaffold (SmartBone®) for maxillary sinus augmentation: a histologic study on bone regeneration

Delfo D'Alessandro[1], Giuseppe Perale[2,3], Mario Milazzo[4], Stefania Moscato[5], Cesare Stefanini[4,6], Gianni Pertici[2,3], Serena Danti[1,4,7,*]

[1] *Dept. of Surgical, Medical, Molecular Pathology and Emergency Medicine, University of Pisa, via Paradisa 2, 56124 Pisa, Italy.*

[2] *Dept. of Innovative Technologies, University of Applied Sciences and Arts of Southern Switzerland (SUPSI), via Cantonale 2C, 6928 Manno, Switzerland.*

[3] *Industrie Biomediche Insubri S/A (IBI), Via Cantonale 67, CH6805 Mezzovico-Vira, Switzerland.*

[4] *Creative Engineering Design Area, The Biorobotics Institute, Scuola Superiore Sant'Anna, viale R. Piaggio 34, 56025 Pontedera (PI), Italy.*

[5] *Dept. of Clinical and Experimental Medicine, University of Pisa, via Savi 10, 56126 Pisa, Italy*

[6] *Dept. of Biomedical Engineering and Robotics Institute, Khalifa University of Science Technology and Research, P.O. Box 127788, Abu Dhabi, United Arab Emirates.*

[7] *Dept. of Civil and Industrial Engineering, University of Pisa, Largo L. Lazzarino 2, 56122 Pisa, Italy.*

** Correspondence to: Serena Danti, Dept. of Civil and Industrial Engineering, University of Pisa, Largo L. Lazzarino 2, 56122 Pisa, Italy. Tel. Office: +39 050 2217874; Fax (Department): +39 050 2218201. E-mail: s.danti@med.unipi.it*

Ethical statement

The histologic study was conducted using residual samples collected upon routinely procedure for dental implant preparation. Bone samples, routinely removed to create a pilot hole for further implant insertion and subsequently disposed of, were used in this study. The patients signed an informed consent and the material was treated anonymously and in conformity to the principles expressed by the Declaration of Helsinki. As such, an approval from the Ethical Committee is not necessary.

Authors' contributions

DD: designed the study, performed experiments and analyses, interpreted the data and drafted the article; MM: performed experiments and analyses; GP and GP: conceived the study and acquired samples; SM: performed experiments; CS: interpreted the data; SD: designed the study and drafted the article. All the authors gave their approval to the final version.

Conflict of interest

GP and GP declare to be shareholders of IBI S/A. All the other authors declare no conflict of interest.

Keywords

Maxillary bone, tissue engineering, dental implants, histology, scaffold, sinus lift.

Abstract

The ideal scaffold for bone regeneration is required to be highly porous, non-immunogenic, biostable until the new tissue formation, bioresorbable and osteoconductive. This study aimed at investigating the process of new bone formation in patients treated with granular SmartBone® for sinus augmentation, providing an extensive histologic analysis. Five biopsies were collected at 4-9 months post SmartBone® implantation and processed for histochemistry and immunohistochemistry. Histomorphometric analysis was performed. Bone-particle conductivity index (BPCi) was used to assess SmartBone® osteoconductivity.

At 4 months, SmartBone® (12%) and new bone (43.9%) were both present and surrounded by vascularized connective tissue (37.2%). New bone was grown on SmartBone® (BPCi = 0.22). At 6 months, SmartBone® was almost completely resorbed (0.5%) and new bone was massively present (80.8%). At 7 and 9 months, new bone accounted for a large volume fraction (79.3% and 67.4%, respectively) and SmartBone® was resorbed (0.5% and 0%, respectively). Well-oriented lamellae and bone scars, typical of mature bone, were observed. In all the biopsies, bone matrix biomolecules and active osteoblasts were visible. The absence of inflammatory cells confirmed SmartBone® biocompatibility and non-immunogenicity. These data indicate that SmartBone® is osteoconductive, promotes fast bone regeneration, leading to mature bone formation in about 7 months.

1. Introduction

In bone tissue engineering, an ideal scaffold is asked for several key requirements, which must also take into account its specific body location and physiologic tasks. Some requirements are broadly considered fundamental in any osseous reconstruction: namely, non-immunogenicity, sufficient biostability until the formation of mature bone, and high porosity for cell migration, extracellular matrix (ECM) deposition and vascularization (Bose et al., 2012). In addition, the optimal scaffold for bone regeneration should be bioresorbable to permit its substitution with newly formed bone, osteoconductive to attract resident osteoblasts to build new bone, and possibly osteoinductive to induce the osteogenic differentiation of mesenchymal stromal cells (Bose et al., 2012). Every year, over 2 million bone-grafting procedures are performed worldwide for orthopedic treatments, and even more for dental surgery, so that the search for the ideal bone substitute has become more and more specifically tailored to the final application.

Maxillary sinus augmentation is a routinely surgical procedure of bone reconstruction and consolidation by means of grafting materials, which has reached a 90% success rate of dental implant in the mid-term (3-5 years) (Del Fabbro et al., 2004). So far, the autologous bone, often taken from the iliac crest, is considered the gold standard material for bone replacement for its osteoconductive and osteoinductive properties (Burchardt, 1983; van den Bergh et al., 1998; Jensen at al., 1998; Klijn et al., 2010). However, autografting procedures are constrained by some important disadvantages, such as extended surgical time and costs, pain associated to morbidity, resorption unpredictability and limited tissue availability (Burchardt, 1983; Burchardt, 1987; Raghoebar et al., 2001; Klijn et al., 2010). For these reasons, ongoing research efforts are investigating the performance of other biomaterials to be used as bone substitutes in dental surgery.

Among synthetic materials, bioactive glasses, resorbable hydroxyapatite (HA), β-tricalcium phosphate (TCP) and their combinations have been proposed for their similarity to the osseous mineral matrix (Wagner, 1991; Tadjoedin et al., 2000; Artzi et al., 2005; Frenken et al., 2010). Resorbable calcium phosphates own osteoconductive properties and, according to their resorption rates, are progressively substituted by new bone. These materials differ from bone grafts as they do not possess ECM organic molecules, the latter playing a dual role of providing both the structural support for the mineral phase and the stimulatory cues for the resident cells to promote graft remodeling and new bone formation (Simunek et al, 2008). On the other hand, although similar in composition and structure to bone ECM, homo- and xeno-grafts carry the risk of inflammatory and foreign body reactions, and for these reasons they are usually processed to lose their immunogenic properties (Graham et al., 2010).

Among tissue grafts, banked bone from donors represents an interesting alternative to autografts, but ethical constraints, issues on costs, safety and availability have limited its use in oral surgery (van den Bergh et al., 2000; Froum et al., 2006). Therefore, bovine deproteinized (anorganic) bone matrix has become a very popular grafting material for the maxillary floor augmentation owing to its large availability and

reduced costs (Piattelli et al., 1999; Tadjoedin et al., 2003). In such a variegated biomaterials scenario, in which new grafts and their combinations with synthetic biomaterials are proposed as scaffolds for sinus lift procedures, the best clinical choice may be challenging.

A review study conducted in 2009 has reported a 16-year meta-analysis of the English literature about the performance of biomaterials used for sinus floor augmentation (Klijn et al., 2010). This meta-analysis showed that the autologous bone grafting scored the highest total bone volume, thus corroborating to be the gold standard material in sinus lift applications. However, when autologous bone is used for grafting, it is impossible to distinguish between the areas of newly formed and transplanted bone in the tissue biopsies. For this reason, the authors refer to "total bone volume", which is, for autografts, an overestimate of the newly formed bone. Differently, when processed bone grafts and other biomaterials are used, only the new bone is measured (Klijn et al., 2010). This measurement uncertainty is suggestive that other well preforming materials, such as deproteinized bovine bone matrix, could be improved and therefore could move close to the performance of autologous bone. A recent meta-analysis and review study has indeed highlighted that bovine bone grafts and TCP/HA mixtures could be considered second choice substitutes to autologous bone grafting, concluding that comparative histologic studies are still necessary (Corbella et al., 2015).

In addition to the performance uncertainty of the current grafts, extensive histological analyses aimed at disclosing the processes and timeline of new bone formation and graft resorption are not present in literature. Among modified xenografts, a scaffold composed of processed bovine bone matrix reinforced with biopolymers and active agents has recently been proposed as bone substitute for oral surgery, maxillofacial and dental implantology, and is available as a new CE-labeled class III medical device (SmartBone®) (Pertici, 2010). This hybrid material is entitled to have excellent mechanical and bone regeneration properties, proposing to be a great promise for dental and maxillofacial bone tissue engineering (Pertici et al., 2014; Pertici et al., 2015).

This study aimed at performing an extensive histological investigation to assess the biologic processes leading to new bone formation in 5 patients treated with granular SmartBone® for sinus floor augmentation. Histological, immunohistochemical and histormorphometrical analyses, including an osteoconductivity index, were carried out at different times post SmartBone® implantation to assess the quality and quantity of newly formed bone, and to study the process of interaction between this scaffold and the maxillary bone microenvironment. New knowledge on these phenomena could foster the development of advanced scaffolds able to regenerate new bone, which may ultimately provide for the unmet needs in dental and maxillofacial surgery.

2. Materials and Methods

2.1 Sample collection

Biopsies were collected from 5 patients who underwent sinus lift procedure with granular SmartBone® (Industrie Biomediche Insubri S/A, Mezzovico-Vira, Switzerland) prior to dental implant placement. SmartBone® was applied by dental surgeons following the instruction for use, as reported by the manufacturer. Bone samples, routinely removed to create a pilot hole for further implant insertion, were used for this study. These samples were cut with a trephine burr and collected at different time points post SmartBone® implantation, namely 4, 4, 6, 7 and 9 months.

2.2 Sample preparation

Cylinder-like specimens with diameters ranging in 2.0-2.5 mm and lengths up to 6 mm, and plain SmartBone® as control, were fixed in 10% neutral buffered formalin containing 4% formaldehyde w/v (Bio-Optica, Milan, Italy) overnight at 4°C, washed in 1× phosphate-buffered saline (1× PBS) and decalcified in a double distilled water (dd-H_2O) solution of 10% ethylenediaminetetraacetic acid (EDTA, Sigma-Aldrich, St. Louis, MO, USA) at 4°C for 14 days, replacing the solution every 3-4 days. After the decalcification procedure was over, the specimens were dehydrated through immersion in a graded series of ethanol (Sigma-Aldrich)/water (v/v%) solutions: namely, in 70% ethanol for 30 min, in 80% ethanol for 30 min, in 95% ethanol twice, each for 45 min, up into absolute ethanol 3 times, each for 1 h, and finally clarified in xylene (Sigma-Aldrich) twice for 45 min, performing all the steps inside a thermostatic bath set at 40°C. Thereafter, the samples were rinsed in liquid paraffin pre-warmed at 60°C and finally paraffin-embedded. Tissue sections, 6 µm thick were obtained with a standard rotating microtome, mounted on glass slides and stored at 37°C.

Before each staining or reaction, the sections were deparaffinized by soaking them in xylene twice, each for 7 min, and rehydrated in absolute ethanol 3 times, each for 7 min. All these steps were performed at room temperature (RT).

2.3 Histochemical analyses

Histochemical analyses were performed using the following staining and reaction protocols. After each staining or reaction was performed, the samples were dehydrated in absolute ethanol (3 rinses, 5 min each), clarified in xylene (3 rinses, 5 min each) and finally mounted using DPX (Sigma-Aldrich) as a mounting medium. All the steps were performed at RT.

2.3.1 Hematoxylin and Eosin (H&E) staining

H&E was used to highlight cell and tissue morphology. The sections were incubated in hematoxylin solution (Sigma-Aldrich) for 5 min and washed in tap water for 5 min to reveal the staining. The samples were

subsequently incubated in eosin solution (Sigma-Aldrich) for 1 min, quickly rinsed in dd-H_2O and dehydrated as described in section 2.3. All the steps were performed at RT.

2.3.2 Periodic Acid Schiff (PAS) reaction

PAS reaction reveals the glycoproteins in magenta. The sections were incubated in periodic acid (Sigma-Aldrich) diluted to 1% w/v in dd-H_2O for 10 min and. Thereafter, the solution was removed and the sections air dried. Dried sections were incubated in Schiff reagent solution (Sigma-Aldrich) for 15 min. Subsequently, the samples were counterstained in hematoxylin solution for 5 min and washed in tap water for 5 min to reveal the counterstaining. All the steps were performed at RT.

2.3.3 Alcian Blue staining

Alcian Blue staining at pH 2.5 highlights generic glycosaminoglycans (GAGs) in cyan. The sections were incubated in Alcian Blue solutions (kit 04-161802, Bio-Optica, Milan, Italy), according to manufacturer's instructions. Briefly, the sections were incubated in Alcian Blue pH 2.5 solution for 30 min. Thereafter, the staining solution was replaced with the revealing solution for 10 min, and finally the specimens were washed in dd-H_2O for 5 min. Subsequently, the samples were counterstained for 5 min in a dd-H_2O solution containing nuclear fast red (Sigma-Aldrich) diluted to 0.1% w/v and aluminum sulphate (Sigma-Aldrich) diluted to 5% w/v and washed in tap water for 5 min to reveal the counterstaining. All the steps were performed at RT.

2.3.4 Van Gieson staining

Van Gieson staining shows organized collagen fibers in red, whereas other biomolecules in yellow. The sections were first counterstained with hematoxylin solution as described in section 2.3.1, then incubated for 2 min with 1% w/v acid fuchsin (Sigma-Aldrich) in dd-H_2O, diluted to 10% in a picric acid saturated solution (Sigma-Aldrich), and finally washed in dd-H_2O. All the steps were performed at RT.

2.4 Immunohistochemical (IHC) analyses

The sections were permeabilized using Triton X-100 (Sigma-Aldrich) diluted to 0.2% v/v in 1× PBS for 10 min and the quenching of endogenous peroxidases was performed through incubation with 0.6% H_2O_2 (36 volumes) in methanol (Sigma-Aldrich) in the dark for 15 min. To block aspecific binding sites, the samples were incubated with goat serum (Vektor Lab, Burlingame, CA, USA) diluted to 5% v/v in 1× PBS at 37°C for 20 min. Therefore, the sections were incubated with the primary antibodies diluted in a solution composed of bovine serum albumin (BSA, Sigma-Aldrich) diluted to 0.1% in 1× PBS. The slides were placed into a humidified chamber overnight at 4°C. The following antibodies were used: anti-collagen type I, diluted 1:2000 (ab34710, Abcam, Cambridge, MA, USA); anti-osteocalcin, diluted 1:800 (sc30044, Santa Cruz

Biotechnology, Santa Cruz, CA, USA); and anti-TGFβ 1, diluted 1:500 (sc-146, Santa Cruz). After each step, the samples were washed in 1× PBS solution for 10 min. The following day, the specimens were incubated with goat anti-rabbit or goat anti-mouse biotinylated secondary antibodies (Vektor Lab) diluted 1:200 in 1.5% v/v goat serum solution in 1× PBS for 60 min, and subsequently with streptavidin (Vectastain Elite ABC Kit Standard, Vektor Lab) for 30 min, according to manufacturer's instructions. After each step, the samples were quickly rinsed in 0.01% Triton/1× PBS and washed in 1× PBS solutions for 10 min. To reveal the reactions, the sections were incubated in the substrate-chromogen solution 0.5 mg/mL 3,3-diaminobenzidine tetrahydrochloride (DAB, Amresco, Solon, OH, USA), in the dark for 5 min. DAB was activated by adding, immediately before the incubation, 2% v/v of a solution constituted of 1% H_2O_2 36 volumes and dd-H_2O. After 2 washings of 5 min in dd-H_20, the specimens were counterstained with hematoxylin solution for 5 min and washed in tap water for 5 min to reveal the counterstaining. Finally, the sections were dehydrated and mounted as described in 2.3. All the steps were performed at RT, unless otherwise specified. The treated histological sections were observed with a Nikon Eclipse Ci microscope (Nikon Instruments, Amsterdam, The Netherlands) and images were acquired by a digital camera at 200× original magnification.

2.5 Histomorphometric analysis

For each biopsy, histological sections were imaged every 30 µm. Micrographs (*n* = 37, 69, 50, 41 and 34, for samples at months 4, 4, 6, 7, and 9, respectively) were acquired at 200× original magnification with a resolution of 2048×1536 pixels to obtain single complete photographic reconstructions of the sections. The different micrograph numericity depended on the different size of biopsies. The histomorphometric study was aimed at estimating the surface percentage occupied by SmartBone®, new bone, connective tissue and other tissues. The different areas in the images, preliminary identified by expert histologists, were manually selected and analyzed using ImageJ software (version 1.50i; http://imagej.nih.gov), using the function "Measure" with "Freehand" selection tool. Briefly, in each micrograph the different tissue areas and the total micrograph area, the latter subtracted from possible empty zones derived by histologic processing, were measured in pixels by the software, thus allowing the percent areas occupied by SmartBone®, new bone, connective tissue and other tissues to be calculated without the need to be converted to the scale bar units. For each patient, the mean percent values of the different areas were obtained as an average over the number of micrographs analyzed. Finally, the mean percentages of the areas occupied by SmartBone®, new bone, connective tissue and other tissues, representative of the volumes analyzed, were given as volumes, considering that the section thickness is much smaller than the section area.

Furthermore, the contribution of SmartBone® particles to new bone formation was evaluated using the Bone-Particle Conductivity Index (BPCi), defined as

$$BPCi = L_c/P_c$$

In which L_C is the sum of contact lengths between new bone and SmartBone® particles and P_S is the sum of perimeters of SmartBone® particles, measured via ImageJ software using the function "Measure" with "Freehand" selection tool. This index ranges from 0, when new bone is not present (only SmartBone® is present), to an indefinite value, when SmartBone® particles are completely absorbed by the host tissues.

3. Results and Discussion

The ideal scaffold for bone regeneration is required to be highly porous, non-immunogenic, biostable until the new tissue formation, bioresorbable and osteoconductive. Among the wide number of biomaterials used for sinus lift in dental surgery, SmartBone® is a new hybrid bone substitute composed by deproteinized bovine spongy bone, a biodegradable copolymer (PLCL) and gelatin.

This study aimed at investigating the process of new bone formation in 5 patients treated with granular SmartBone® for sinus augmentation, providing an extensive histologic analysis, which is necessary to understand the underlying mechanisms driving the biological phenomena at the basis of graft acceptance, resorption, quality and quantity of new bone formation. Understanding these aspects is fundamental to accelerate the development of novel materials for bone tissue engineering.

3.1 Histological analysis

Many authors have reported on the outcomes of different materials used in sinus lift procedures, which included histological analyses of biopsies performed on reconstructed maxillary bone. These analyses were mainly carried out to evaluate the material resorption and the presence of new bone tissue using H&E or Toluidine Blue staining, alone or in combination with Trichromic staining, the latter to reveal collagen fibers (Galindo-Moreno et al., 2008; Soardi et al., 2011; Spin-Neto et al., 2014). However, these histologic methods cannot give specific and deepen information on the localization and expression bone ECM biomolecules, which in our opinion are greatly important to assess the process leading to formation and maturity of newly formed bone. For these reasons, we performed an extensive histological analysis on sinus biopsies, consisting in histochemical staining/reaction and IHC reactions performed against specific bone ECM antigens.

The histological analysis using H&E was firstly performed to understand the timeline of new bone formation and SmartBone® resorption in the 5 tissue samples, collected at different time points **(Figure 1)**. At 4 months after implantation, both SmartBone® and new bone could be easily identified, due to absence and presence of cells inside bone lacunae, respectively **(Figure 1 A, B)**. Differently, starting from month 6,

SmartBone® was rarely observed, indicating that its resorption had already occurred **(Figure 1 C-E)**. H&E performed on plain SmartBone® showed that the graft structure maintained the morphological features typical of bone tissue. In particular, empty bone lacunae, i.e. not occupied by osteocytes, were clearly observed, indicating complete graft decellularization **(Figure 1 F)**. From our panel of analyses, SmartBone® resulted unevenly weakly positive to collagen fibers, generic GAGs, glycoproteins, collagen type I and fibronectin, the latter specifically located around the bone lacunae, while it was negative to TGF-β1. These results are in line with the non-aggressive deproteinization, as declared by the manufacturer (data not shown) (Pertici et al., 2014).

A representative biopsy at 4 months (biopsy #1) was chosen to show an extensive characterization of the tissue **(Figure 1A, 2)**. SmartBone® stained with less intensity than new bone and its bone lacunae did not contain any osteocytes, thus allowing its easy identification in the histologic sections. In contrast, new bone areas showed osteocytes housed in the bone lacunae and osteoblasts layering at the periphery of new bone grown on SmartBone®, which is highly suggestive of good material osteoconductivity. The connective tissue around bone and SmartBone® areas appeared well-structured, was in contact with SmartBone® and contained blood vessels, indicating acceptance and integration of the graft material in the recipient site **(Figure 1 A)**. Areas with some cellular infiltration could be very rarely observed. The co-existence of bovine graft material and new bone at 4 months is in agreement with the literature, although the data reported at such an early time point are limited (Wheeler et al., 1997). PAS reaction highlighted good positivity for glycoproteins in the new bone, mainly along the growth line in contact with SmartBone®, which conversely appeared negative **(Figure 2 A)**. Generic GAGs were localized mainly around the bone lacunae and, with less intensity, along the bone lamellae in the new bone, whereas SmartBone® was weakly positive only around the empty bone lacunae **(Figure 2 B).** Collagen fibers were well evident in the bone lamellae of new bone. SmartBone® showed a weak positivity to Van Gieson staining, possibly indicating the presence of degraded collagen **(Figure 2 C).** IHC analysis revealed an intense positivity for collagen type I in the new bone **(Figure 2 D).** Differently, osteocalcin was detected mainly along bone lamellae at the periphery of the new bone areas **(Figure 2 E)**. Moreover, TGF-β1 specifically highlighted osteoblasts located along the margins of the new bone **(Figure 2 F)**. Briefly, in the 4-month biopsy, both SmartBone® and new bon tissue were present; new bone grew on SmartBone® and well-structured vascularized connective tissue surrounded both new bone and SmartBone®. As a proof of cytocompatibility, preliminary in vitro studies conducted by culturing human mesenchymal stromal cells on SmartBone® cubes for 3 weeks without any osteogenic supplements showed that the cells were viable, colonized the scaffold and produced generic GAGs **(Figures S1 and S2 – Supplementary)**. All these data and the almost total absence of inflammatory cells in the biopsies confirmed that this material is highly biocompatible (Pertici et al., 2015).

From 6 months ahead, SmartBone® started to be completely resorbed and only new bone areas were visible. These results are different from those using ceramic substitutes, in which resorption at 6 months

was still partial (Frenken et al., 2010). In the 6-month biopsy, large new bone areas containing osteocytes in bone lacunae were observed, whereas SmartBone® particles were extremely rare **(Figure 1 C).** In similar studies with bone block allografts, the histological analyses at 6 months showed that the graft materials were still present (Nissan et al., 2011; Spin-Neto et al., 2014), thus indicating that SmartBone® was able to accelerate new bone formation. In new bone areas, a good positivity for glycoproteins was shown and a strong presence of generic GAGs was revealed in the ECM surrounding the bone lacunae **(Figure 3 A, B).** Collagen fibers were well represented along both the bone lamellae and the bone lacunae **(Figure 3 C).** Collagen type I and osteocalcin were detected mainly at the periphery of the bone areas **(Figure 3 D,E)**. In this biopsy, TGF-β1 was not revealed by IHC analysis **(Figure 3 F)**.

In the 7-month biopsy, well oriented bone lamellae were visible and the presence of some bone scars, typical of mature bone, could be observed, whereas SmartBone® was very rarely detected **(Figure 1 D, 4)**. These results are remarkably different from those found in the literature. In these studies, histological analyses on implanted bovine-derived bone grafts, such as Bio-Oss®, displayed the co-existence of graft material and new bone in 7-month biopsies, reporting newly formed bone, growth around the graft, with diverse maturity levels (Yildirim et al., 2000; Froum et al., 2008). In contrast, the new bone found in our samples appeared highly mature. The glycoproteins were intensely expressed along bone lamellae and in the bone scars **(Figure 4 A)**. Good positivity for generic GAGs was revealed around bone lacunae, whereas it was weak along bone lamellae **(Figure 4 B)**. Van Gieson staining highlighted well oriented collagen fibers in the bone lamellae **(Figure 4 C)**. High levels of expression for collagen type I and osteocalcin were detected in the bone lamellae **(Figure 4 D, E)**. Finally, TGF- β1 was strongly expressed in the osteoblasts at the margins of new bone **(Figure 4 F)**.

In the 9-month biopsy, new bone areas containing osteocytes in the bone lacunae and many bone scar lines were imaged, while SmartBone® was absent **(Figure 1 E)**. Glycoproteins were well expressed mainly in the bone scars **(Figure 5 A)**. Good positivity for generic GAGs was shown around the bone lacunae **(Figure 5 B)**. Well oriented collagen fibers were detected and collagen type I was observed along the bone lamellae **(Figure 5 C, D).** In a similar fashion, osteocalcin was well expressed in the bone areas **(Figure 5 E)**. Weak TGF- β1 expression was observed in the cells located along the margin of the bone tissue **(Figure 5 F)**.

In all the biopsies, the presence of the most important bone ECM biomolecules, such as glycoproteins, generic GAGs and collagen fibers, was assessed. The progression of bone biomolecule expression along the time, as well as the appearance of specific morphologic features of mature bone, like oriented bone lamellae and bone scars, indicated that around 6 months after implantation, the newly formed bone tissue was mature. Month 6 seemed to be a turning point, as Smartbone® was also almost fully resorbed. The presence of many osteoblasts along the margins of new bone, observed in all the biopsies, indicated that new bone formation process is well underway. In a comparative study between anorganic bovine matrix (Bio-Oss®) and a mineralized cancellous bone allograft (Puros®), a significant new bone amount was formed

in patients implanted with Puros®, which may suggest a fundamental role played by the co-existence of both mineral and organic bone ECM in bone regeneration (Froum et al., 2006). SmartBone® is a hybrid scaffold designed to have an improved performance with respect to those of other anorganic xenografts, by using deproteinized bovine bone combined with biocompatible and bioresorbable biopolymers, such as PLCL and gelatin. The graft part of SmartBone® is harvested from bovine bone and treated via acid attack at low temperature (Pertici, 2010; Pertici et al., 2014). This process is performed to mildly remove the organic matrix from the xenograft, thus reaching non-immunogenicity while preserving the chemical structure of the mineral phase. As a consequence, the final scaffold can undergo complete remodeling, as also corroborated by our observations in the 9-month biopsy. As soon after surgery, the added biopolymers are specifically designed to improve the volumetric stability of the granular graft. Gelatin increases the graft wettability, which ultimately leads to the formation of a paste, easy to manage, due to rapid and deep blood absorption, which enables the recruitment of neighboring cells into the scaffold, thus stimulating bone cell adhesion and proliferation. Other porous biodegradable spongy scaffolds based on poly(L-lactic acid) (PLA) and gelatin were proven to be blood compatible, support osteoblast adhesion and allow the formation of osteogenic niches (Lazzeri et al., 2007; Danti et al. 2007; Danti et al. 2012). The addition of biopolymers and gelatin to deproteinized bovine graft is hypothesized to be a key feature to activate the processes of new bone formation and graft resorption in such a short time frame.

3.2 Histomorphometric analysis

Histomorphometric analysis is a software-aided tool for the quantitative evaluation of histologic specimens, which enables a robust understanding of bone formation versus graft resorption and permits comparisons among samples (Egan et al., 2012). In a meta-analysis review, Klijn and coworkers carried out a systematic evaluation of the effects played by material, biopsy time, technique (block or particulated grafting), collagen membrane (presence or absence), and implant strategy (immediate or delayed), on the amount of total bone volume detected by histomorphometric analysis (Klijn et al. 2010). This study showed that grafting type, time of biopsy collection and strategy of implant placement were all significant variables on the histomorphometric outcomes for many biomaterials. We thus evaluated the histomorphometric results obtained with SmartBone® , comparing them to those reported for similar materials (deproteinized bovine matrices). We also compared similar/higher histomorphometric results of different materials to those obtained using SmartBone®. In these comparisons, we considered these specific variables: biopsy times, particulate grafting, presence of a collagen membrane and delayed implant.

The results of volume percentages of new bone, SmartBone®, connective and other tissues obtained in our samples via histomorphometric analysis are reported in **Figure 6.** In the two biopsies at 4 months after SmartBone® implant, the new bone volume averagely accounted for 43.9% (40.3%-47.5% range) of the total sample volume. At that time point, particulate SmartBone® was already massively resorbed, being

detected on average at 12% (10.5%-12.5% range). Connective tissue still averagely covered 37.2% (37.0%-37.4% range) of the total volume **(Figure 6 A,B)**. The literature on 4-month biopsies is very limited, as they are usually carried out at later time points. Wheeler and colleagues reported on 4 sinus biopsies obtained at 4 months after implantation of Interpore® 200, an anorganic deproteinized bovine bone grafts, in which the bone volume accounted for 12.02% (Wheeler at al., 1996). Another study on 3 sinuses performed at 4 months using particulate autograft (namely, the gold standard material), but in absence of collagen membrane, showed 40.94% of total bone volume, which may be comparable to the results obtained using SmartBone® (Tadjoedin et al., 2000). A similar outcome was reported using anorganic deproteinized bovine bone particles (Bio-Oss®) mixed with autologous bone graft in 2 sinuses at 12 months post implantation (45.6% bone volume) (Artzi et al., 2005). These comparisons, even though conducted on limited biopsy numbers, are strongly suggestive of the highest SmartBone® performance with respect to those of anorganic bovine bone substitutes. The rate of new bone formation appears to be induced by biological phenomena occurring at early times post implantation, thus highlighting that the hybrid composition really makes a difference.

At 6 and 7 months, Smartbone® particles were rarely present (0.5%), new bone covered almost completely the sample areas with volume percentages of 80.8% and 79.3%, respectively, and connective tissue was reduced to 18.7% and 20.2%, respectively **(Figure 6 C, D)**. Such high bone volumes in sinus augmentation, specifically 70.0% and 69.7%, have solely been shown using particulate autografts as maxillary fillers at 5 months, under the same variables mentioned above (Barone et al. 2005; Crespi et al., 2007). In fact, results at 6 months using anorganic deproteinized bovine bone (Bio-Oss®) showed only 13.5% and 18.30% new bone volumes (Yildirim et al., 2000; Lee et al., 2006), and 22.3% just after the 7^{th} month (Froum et al. 2008). At 9 months post SmartBone® implant, the new bone volume accounted for 67.4%, connective tissue for 25.6% and other tissues for 7.0%. SmartBone® was never detected in this biopsy (0%) **(Figure 6 E)**. At the same time point and variable conditions, implanted Bio-Oss® was reported to have induced just 16.5% bone volume (Yildirim et al., 2000).

To improve the comprehension of the mechanisms leading to new bone formation and SmartBone® resorption, we evaluated an osteoconductivity index, specifically the BPCi. This index measures the contact between the new bone and material particles, thus being a tool to assess osteoconductivity. It has to be underlined that, in case of a resorbable particulate, this index is affected by two competitive kinetics, the material resorption velocity and the bone growth velocity. Moreover, for its constitutive definition, the BPCi ranges from 0 (only material particles) to indefinite (only new bone). As such, it can be measured only when the material particles are present. In the 4-month biopsies, the BPCi resulted to range in 19.1%-25.3%, indicating that averagely 22.2% of the SmartBone® areas were in contact with newly formed bone. In the biopsies at later time points (6 and 7 months), the quantity of SmartBone was so small (0.5% in volume) that BPCi was very difficult to evaluate. At 9 month, SmartBone® was no more detectable, making

BPCi indefinite. From these preliminary evaluations, also corroborated by the histological outcomes, it can be stated that SmarBone® owns good osteoconductivity, although shorter time points (< 4 months) are necessary to define the role and entity of osteoconductivity on the process of new bone formation driven by SmartBone®.

SmartBone® is an innovative bone substitute composed by bovine spongy bone, which is deproteinized via a mild acid attack process to preserve the graft structure, and ultimately added with PLCL as a biodegradable copolymer and gelatin to improve its volumetric stability and wettability at the onset of implantation. Gelatin was also chosen to offer RGD-sequences to cells in order to better support their adhesion and spreading. This hybrid formulation leads to the formation of a paste, due to rapid and deep blood absorption, which recruits the neighboring cells to get into the scaffold. This peculiarity seems to be a key feature to activate very soon the processes of new bone formation and graft resorption.

4. Conclusions

Upon SmartBone® implantation for sinus lift, in the 4-month biopsies, new bone was largely present (43.9%) and partially in contact with the residual SmartBone® (12%), which was already partially resorbed (BPCi = 0.22). The new bone volume was comparable to the total bone volume measured at 4 months using bone autografts, which is the gold standard material for this procedure. Other anorganic xenografts scored much lower values at the same time point, or needed, even if mixed with bone autografts, much longer times to reach similar results. At 6 months, the residual SmartBone® was very small (0.5%) and new bone was massively present (80.8%), a result comparable only to some outcomes obtained using particulate bone autografts. At 7 and 9 months, SmartBone® was 0.5% and 0%, respectively, and well-oriented lamellae and bone scars, typical of mature bone, were observed. Bone matrix biomolecules and active osteoblasts, positive for TGF-β1, were very often visible. The absence of inflammatory cells confirmed SmartBone® biocompatibility and non-immunogenicity. Even though these data are obtained on a limited number of patients and shorter time points would be necessary to completely understand the biological phenomena occurring in the very early stages of new bone formation, the obtained outcomes showed that SmartBone® is osteoconductive, promotes fast bone regeneration, leading to mature bone formation in about 7 months.

Acknowledgements

The authors kindly acknowledge Dr. Armando Minciarelli (Bari), Dr. Roberto Pezzoli (Casnigo, BG), Dr. Fabrizio Secondo (Collegno, TO) and Dr. Federico Mandelli (Pioltello, MI) (Italy) for sample collection. Many

thanks are due to Mr. Andrea Mari and Dr. Luisa Trombi, University of Pisa (Italy), for their technical contribution to histomorphometric analysis and in vitro culture (Supplementary material), respectively.

References

Artzi, Z., Kozlovsky, A., Nemcovsky, C.E., Weinreb, M., 2005. The amount of newly formed bone in sinus grafting procedures depends on tissue depth as well as the type and residual amount of the grafted material. J. Clin. Periodontol. 32, 193-199.

Barone, A., Crespi, R., Aldini, N.N., Fini, M., Giardino, R., and Covani, U., 2005. Maxillary sinus augmentation: histologic and histomorphometric analysis. Int. J. Oral Maxillofac. Implants 20, 519-525.

Bose, S., Roy, M., Bandyopadhyay, A., 2012. Recent advances in bone tissue engineering scaffolds. Trends Biotechnol. 30, 546-554.

Burchardt, H., 1983. The biology of bone graft repair. Clin. Orthop. Relat. Res. 174, 28-42.

Burchardt, H., 1987. Biology of bone transplantation. Orthop. Clin. North Am. 18, 187-196.

Corbella, S., Taschieri, S., Weinstein, R., Del Fabbro, M., 2015. Histomorphometric outcomes after lateral sinus floor elevation procedure: a systematic review of the literature and meta-analysis. Clin. Oral Implants Res. *In press.*

Crespi, R., Vinci, R., Cappare, P., Gherlone, E., and Romanos, G.E., 2007. Calvarial versus iliac crest for autologous bone graft material for a sinus lift procedure: a histomorphometric study. Int. J. Oral Maxillofac. Implants 22, 527-532.

Danti, S., Rizzo, C., Polacco, G., Cascone, M.G., Giusti, P., Lisanti, M., 2007. Design of an advanced temporary hip prosthesis for an effective recovery of septic mobilizations: a preliminary study. Int. J. Artif. Organs. 30, 939-949.

Danti, S., Serino, L.P., D'Alessandro, D., Moscato, S., Danti, S., Trombi, L., Dinucci, D., Chiellini, F., Pietrabissa, A., Lisanti, M., Berrettini, S., Petrini, M., 2013. Growing bone tissue-engineered niches with graded osteogenicity: an in vitro method for biomimetic construct assembly. Tissue Eng. Part C Methods. 19, 911-924.

Del Fabbro, M., Testori, T., Francetti, L., Weinstein, R., 2004. Systematic review of survival rates for implants placed in the grafted maxillary sinus. Int. J. Periodontics Restorative Dent. 24, 565-577.

Egan, K.P., Brennan, T.A., Pignolo, R.J., 2012. Bone histomorphometry using free and commonly available software. Histopathology. 61, 1168-1173.

Frenken, J.W., Bouwman, W.F., Bravenboer, N., Zijderveld, S.A., Schulten, E.A., ten Bruggenkate, C.M., 2010. The use of Straumann Bone Ceramic in a maxillary sinus floor elevation procedure: a clinical, radiological, histological and histomorphometric evaluation with a 6-month healing period. Clin. Oral Implants Res. 21: 201-218.

Froum, S.J., Wallace, S.S., Cho, S.C., Elian, N., Tarnow, D.P., 2008. Histomorphometric comparison of a biphasic bone ceramic to anorganic bovine bone for sinus augmentation: 6- to 8-month postsurgical assessment of vital bone formation. A pilot study. Int. J. Periodontics Restorative Dent. 28, 273-281.

Froum, S.J., Wallace, S.S., Elian, N., Cho, S.C., Tarnow, D.P., 2006. Comparison of mineralized cancellous bone allograft (Puros) and anorganic bovine bone matrix (Bio-Oss) for sinus augmentation: histomorphometry at 26 to 32 weeks after grafting. Int. J. Periodontics Restorative Dent. 26, 543-551.

Galindo-Moreno, P., Avila, G., Fernández-Barbero, J.E., Mesa, F., O'Valle-Ravassa, F., Wang, H.L., 2008. Clinical and histologic comparison of two different composite grafts for sinus augmentation: a pilot clinical trial. Clin. Oral Implants Res. 19, 755-759.

Graham, S.M., Leonidou, A., Aslam-Pervez, N., Hamza, A., Panteliadis, P., Heliotis, M., Mantalaris, A., Tsiridis, E., 2010. Biological therapy of bone defects: the immunology of bone allo-transplantation. Expert Opin. Biol. Ther. 10, 885-901.

Jensen, O.T., Shulman, L.B., Block, M.S., Iacono, V.J., 1998. Report of the Sinus Consensus Conference of 1996. Int. Oral Maxillofac. Implants. 13, 11-45.

Klijn, R.J., Meijer, G.J., Bronkhorst, E.M., Jansen, J.A., 2010. A meta-analysis of histomorphometric results and graft healing time of various biomaterials compared to autologous bone used as sinus floor augmentation material in humans. Tissue Eng. Part B Rev. 16, 493-507.

Lazzeri, L., Cascone, M.G., Danti, S., Serino, L.P., Moscato, S., Bernardini, N., 2007. Gelatine/PLLA sponge-like scaffolds: morphological and biological characterization. J. Mater. Sci. Mater. Med. 18, 1399-1405.

Lee, Y.M., Shin, S.Y., Kim, J.Y., Kye, S.B., Ku, Y., Rhyu, I.C., 2006. Bone reaction to bovine hydroxyapatite for maxillary sinus floor augmentation: histologic results in humans. Int. J. Periodontics Restorative Dent. 26, 471-481.

Nissan, J., Marilena, V., Gross, O., Mardinger, O., Chaushu, G., 2011. Histomorphometric analysis following augmentation of the posterior mandible using cancellous bone-block allograft. J. Biomed. Mater. Res. A. 97, 509-13.

Pertici, G., 2010. Bone implant matrix and method of preparing the same. Patent WO2010070416A1.

Pertici, G., Carinci, F., Carusi, G., Epistatus, D., Villa, T., Crivelli, F., Rossi, F., Perale, G., 2015. Composite polymer-coated mineral scaffolds for bone regeneration: from material characterization to human studies. J. Biol. Regul. Homeost. Agents. 29, 136-148.

Pertici, G., Rossi, F., Casalini, T., Perale, G., 2014. Composite polymer-coated mineral grafts for bone regeneration: material characterization and model study. Annals of Oral & Maxillofacial Surgery. 14, 1-7.

Piattelli, M., Favero, G.A., Scarano, A., Orsini, G., Piattelli, A., 1999. Bone reactions to anorganic bovine bone (Bio-Oss) used in sinus augmentation procedures: a histologic long-term report of 20 cases in humans. Int. J. Oral Maxillofac. Implants. 14, 835-840.

Raghoebar, G.M., Louwerse, C., Kalk, W.W., Vissink, A., 2001. Morbidity of chin bone harvesting. Clin. Oral Implants Res. 12, 503-507.

Simunek, A., Kopecka, D., Somanathan, R.V., Pilathadka, S., Brazda, T., 2008. Deproteinized bovine bone versus β-tricalcium phosphate in sinus augmentation surgery: a comparative histologic and histomorphometric study. Int. J. Oral Maxillofac. Implants. 23, 935-942.

Soardi, C.M., Spinato, S., Zaffe, D., Wang, H.L., 2011. Atrophic maxillary floor augmentation by mineralized human bone allograft in sinuses of different size: an histologic and histomorphometric analysis. Clin. Oral Implants Res. 22: 560-566.

Spin-Neto, R., Stavropoulos, A., Coletti, F.L., Faeda, R.S., Pereira, L.A., Marcantonio, E. Jr., 2014. Graft incorporation and implant osseointegration following the use of autologous and fresh-frozen allogeneic block bone grafts for lateral ridge augmentation. Clin. Oral Implants Res. 25, 226-233.

Tadjoedin, E.S., de Lange, G.L., Bronckers, A.L., Lyaruu, D.M., Burger, E.H., 2003. Deproteinized cancellous bovine bone (Bio-Oss) as bone substitute for sinus floor elevation. A retrospective, histomorphometrical study of five cases. J. Clin. Periodontol. 30, 261-270.

Tadjoedin, E.S., de Lange, G.L., Holzmann, P.J., Kulper, L., Burger, E.H., 2000. Histological observations on biopsies harvested following sinus floor elevation using a bioactive glass material of narrow size range. Clin. Oral Implants Res. 11, 334-344.

van den Bergh, J.P., ten Bruggenkate, C.M., Krekeler, G., Tuinzing, D.B., 2000. Maxillary sinusfloor elevation and grafting with human demineralized freeze dried bone. Clin. Oral Implants Res. 11, 487-493.

van den Bergh, J.P., ten Bruggenkate, C.M., Krekeler, G., Tuinzing, D.B., 1998. Sinusfloor elevation and grafting with autogenous iliac crest bone. Clin. Oral Implants Res. 9: 429-435.

1 Wagner, J.R., 1991. A 3 1/2-year clinical evaluation of resorbable hydroxylapatite OsteoGen (HA Resorb)
2 used for sinus lift augmentations in conjunction with the insertion of endosseous implants. J. Oral
3 Implantol. 17, 152-64.

4 Wheeler, S.L., Holmes, R.E., Calhoun C.J., 1996. Six-year clinical and histologic study of sinus-lift grafts. Int. J.
5 Oral Maxillofac. Implants. 11, 26-34.

6 Yildirim, M., Spiekermann, H., Biesterfeld, S., Edelhoff, D., 2000. Maxillary sinus augmentation using
7 xenogeneic bone substitute material Bio-Oss® in combination with venous blood. Cli. Oral impl. Res. 11,
8 217-229.

9

Figure legends

Figure 1. H&E staining of maxillary bone biopsies and pristine SmartBone® material. **(A)** Biopsy #1 at 4 months. **(B)** Biopsy #2 at 4 months. **(C)** Biopsy at 6 months. **(D)** Biopsy at 7 months. **(E)** Biopsy at 9 months. **(F)** Plain SmartBone® material. **(A-F)** Original magnification ×200. NB = new bone; SB = SmartBone®; CT = connective tissue; gl = growth line; V = blood vessels; black arrow = bone lacunae; red arrow = bone scar; black arrowhead = osteoblasts; red arrowheads = bone lamellae.

Figure 2. Histological analyses of a representative biopsy at 4 months (biopsy #1). **(A)** PAS reaction reveals the presence of glycoproteins in magenta. **(B)** Alcian Blue staining at pH 2.5 shows generic GAGs in cyan. **(C)** Van Gieson staining reveals collagen fibers in new bone areas in red. Non-collagenic elements are stained in yellow. Cell nuclei are stained in black. **(D)** IHC analysis shows collagen type I localization. **(E)** IHC analysis reveals osteocalcin. **(F)** TGF-β1 is detected via IHC**. (A-E)** Original magnification ×200. **(F)** Original magnification ×400. **(A-F)** NB = new bone; SB = SmartBone®; CT = connective tissue; gl = growth line; black arrow = bone lacunae; black arrowheads = osteoblasts; red arrowheads = bone lamellae.

Figure 3. Histological analyses on the biopsy at 6 months. **(A)** PAS reaction shows the glycoproteins in magenta. **(B)** Alcian Blue at pH 2.5 reveals generic GAGs in cyan. **(C)** Van Gieson staining shows collagen fibers in red. Non-collagenic elements are stained in yellow. Cell nuclei are in black. **(D)** IHC analysis reveals collagen I. **(E)** IHC analysis shows osteocalcin localization. **(F)** IHC reaction is negative for TGF-β1. **(A-E)** Original magnification ×200. **(F)** Original magnification ×400. **(A-F)** Black arrow = bone lacunae; red arrowheads = bone lamellae.

Figure 4. Histological analyses on the biopsy at 7 months. **(A)** PAS reaction shows glycoproteins in magenta; bone scars are visible and intensely positive. **(B)** Alcian Blue at pH 2.5 shows generic GAGs in cyan. **(C)** Van Gieson staining shows collagen fibers in red. Cell nuclei are stained in black. **(D)** IHC analysis detected collagen type I. **(E)** IHC analysis shows osteocalcin. **(F)** TGF-β1 is localized via IHC analysis. **(A-E)** Original magnification ×200. **(F)** Original magnification ×400. **(A-F)** Black arrow = bone lacunae; red arrows = bone scar; black arrowheads = osteoblasts; red arrowheads = bone lamellae.

Figure 5. Histological analyses on the biopsy at 9 months. **(A)** PAS reaction shows glycoproteins in magenta. **(B)** Alcian Blue at pH 2.5 shows generic GAGs in cyan. **(C)** Van Gieson staining reveals collagen fibers in red. Non-collagenic areas are stained in yellow; cell nuclei are stained in black. **(D)** IHC analysis detected collagen type I. **(E)** IHC analysis shows osteocalcin. **(F)** IHC reveals TGF-β1. **(A-E)** Original

magnification ×200. **(F)** Original magnification ×400. **(A-F)** Black arrow = bone lacunae; red arrows = scar bone; black arrowheads = osteoblasts; red arrowheads = bone lamellae.

Figure 6. Histomorphometric analysis showing volume percentages of new bone, SmartBone®, connective tissue, and other tissues in the biopsies taken at the following times post SmartBone® implantation: **(A)** 4 months (Biopsy #1); **(B)** 4 months (Biopsy #2); **(C)** 6 months; **(D)** 7 months; **(E)** 9 months. The results show the timeline of SmartBone® resorption (13.5% to 0%) and new bone formation (ranging in 40.3%-80.8%).

Figure 1

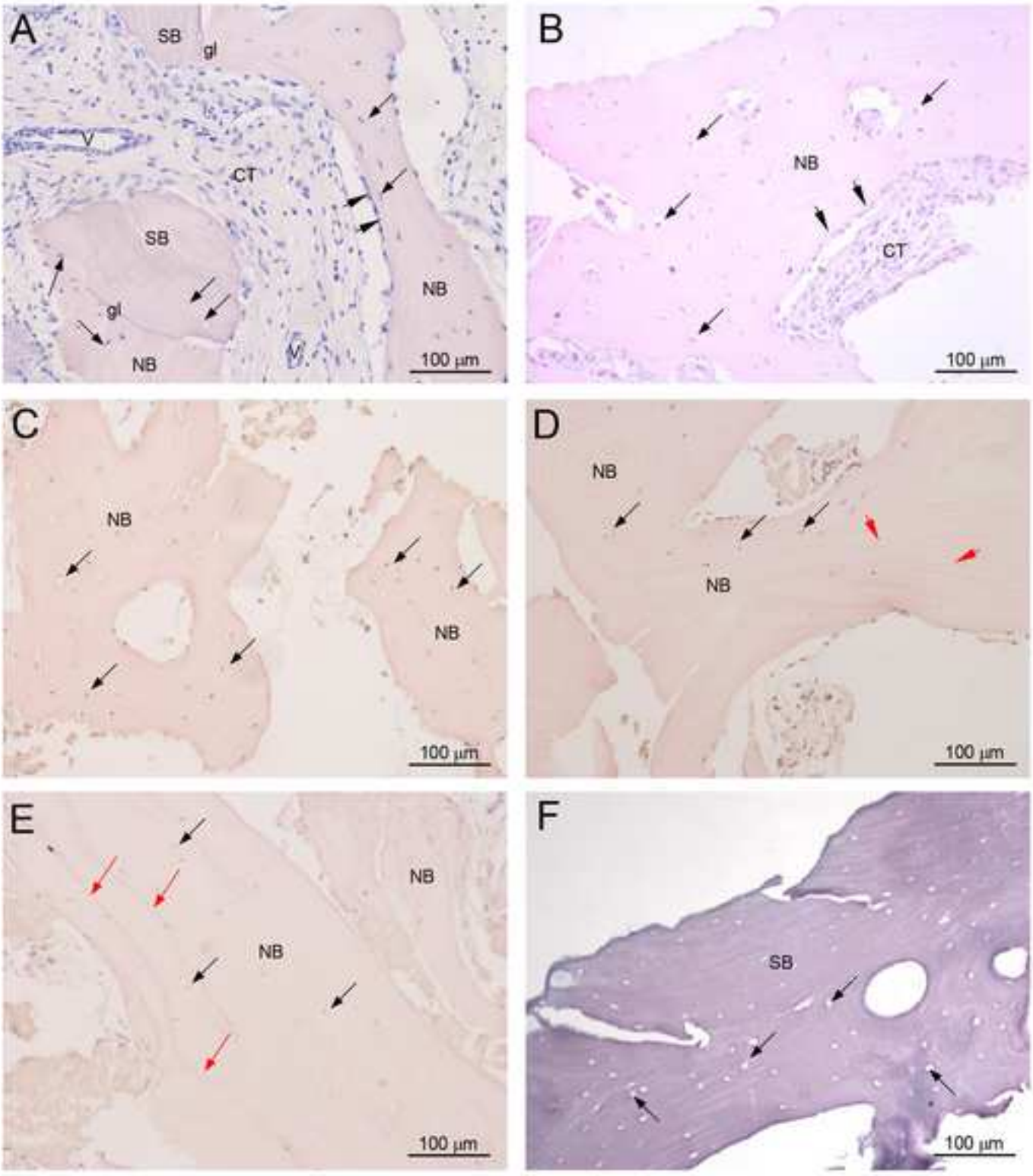
A
SB
gl
V
CT
SB
NB
gl
NB
V
100 µm
B
NB
CT
100 µm
C
NB
NB
100 µm
D
NB
NB
100 µm
E
NB
NB
100 µm
F
SB
100 µm

Figure 2

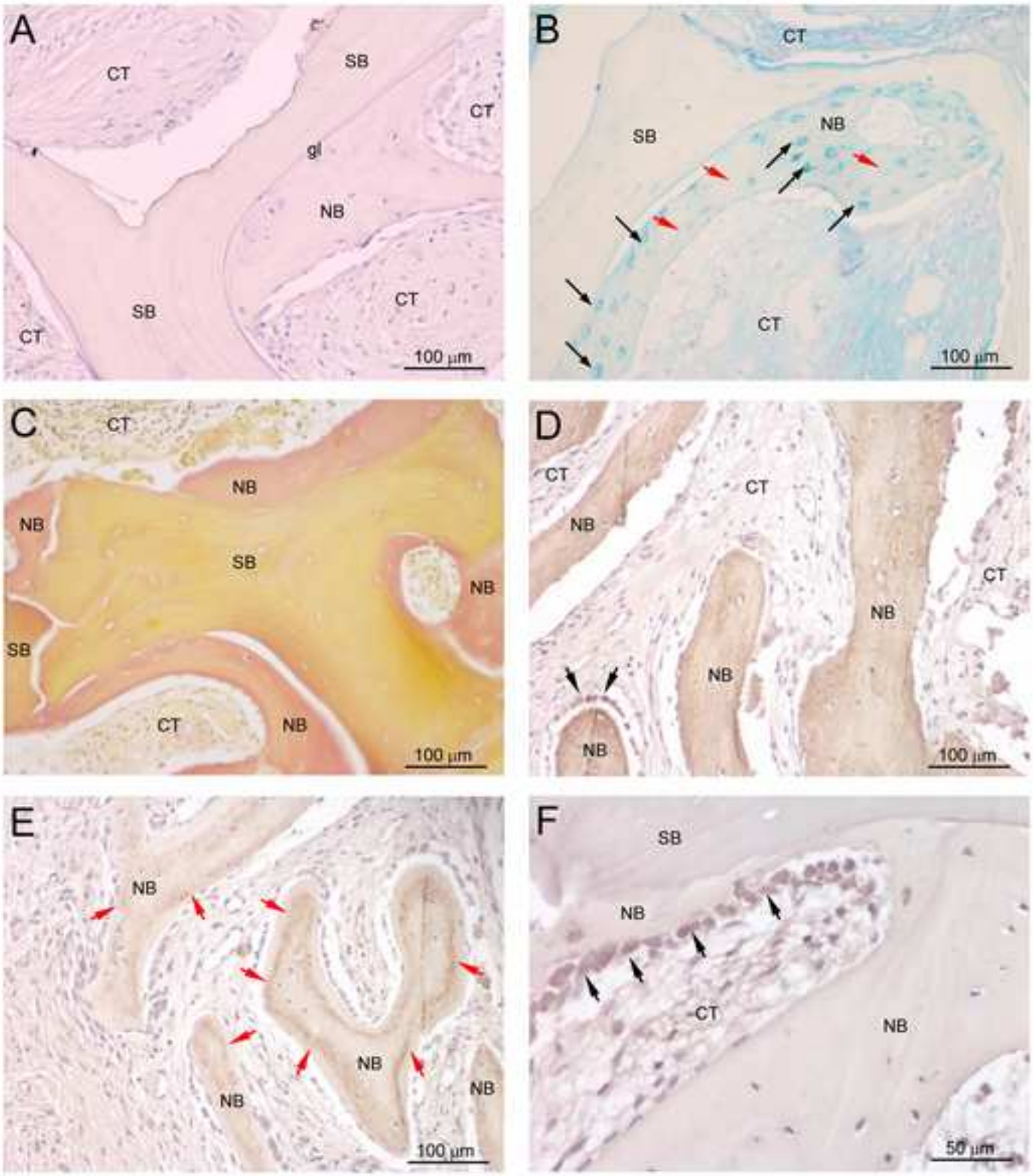
A
CT
SB
CT
gl
NB
SB
CT
CT
100 µm
B
CT
SB
NB
CT
100 µm
C
CT
NB
NB
SB
NB
SB
CT
NB
D
CT
CT
NB
CT
NB
NB
NB
100 µm
E
NB
NB
NB
NB
100 µm
F
SB
NB
CT
NB
50 µm

Figure 3

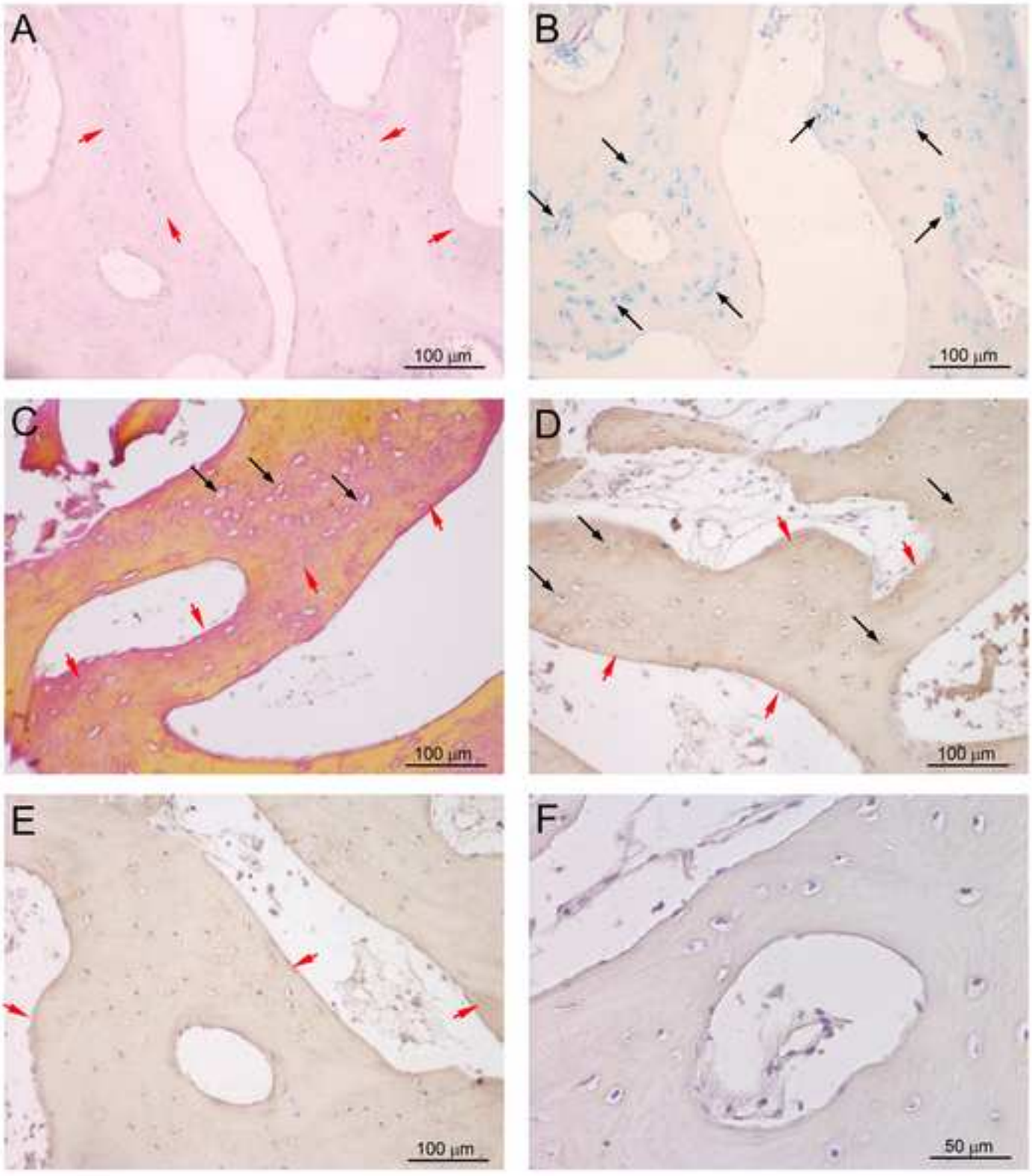

Figure 4

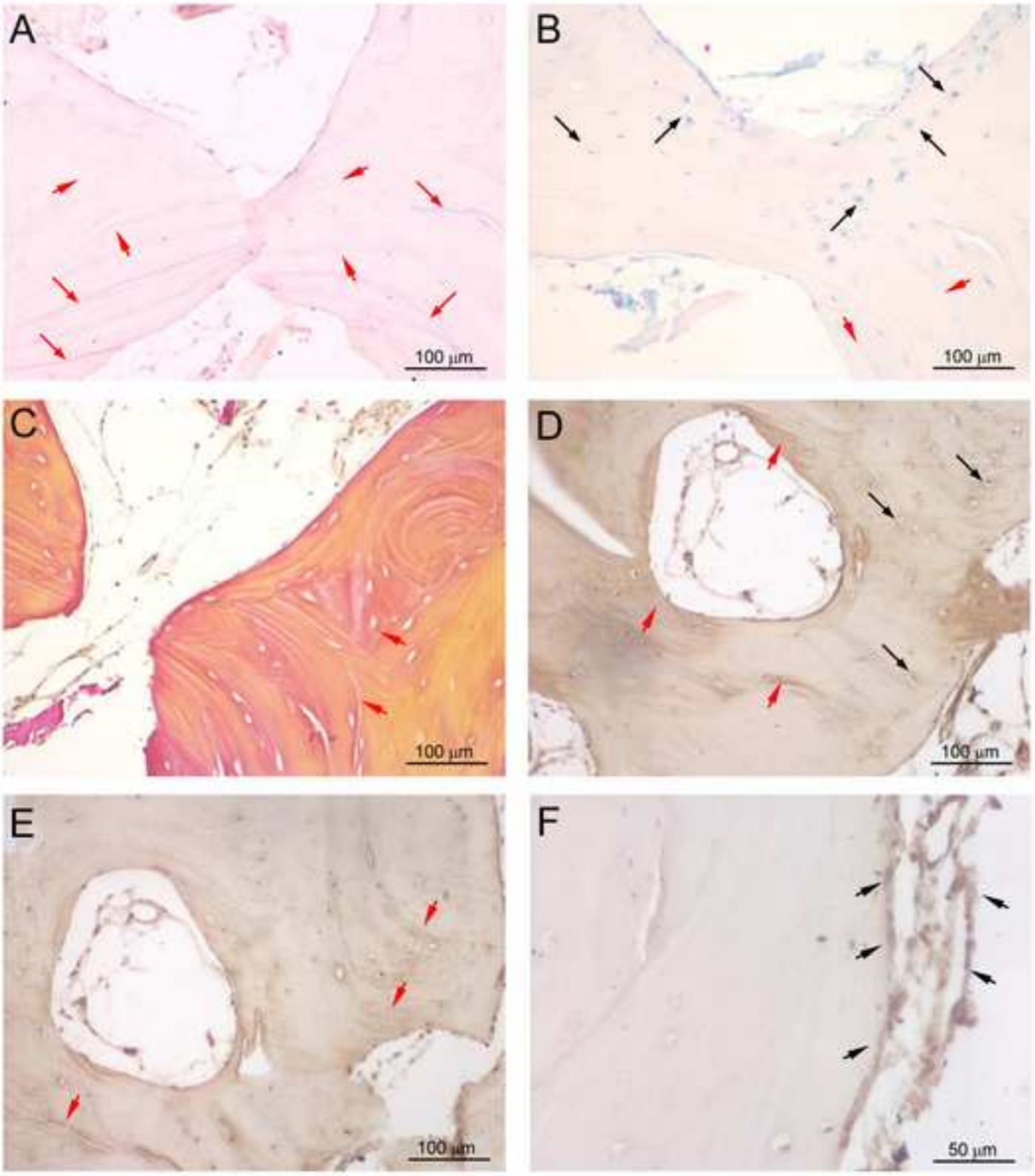

Figure 5

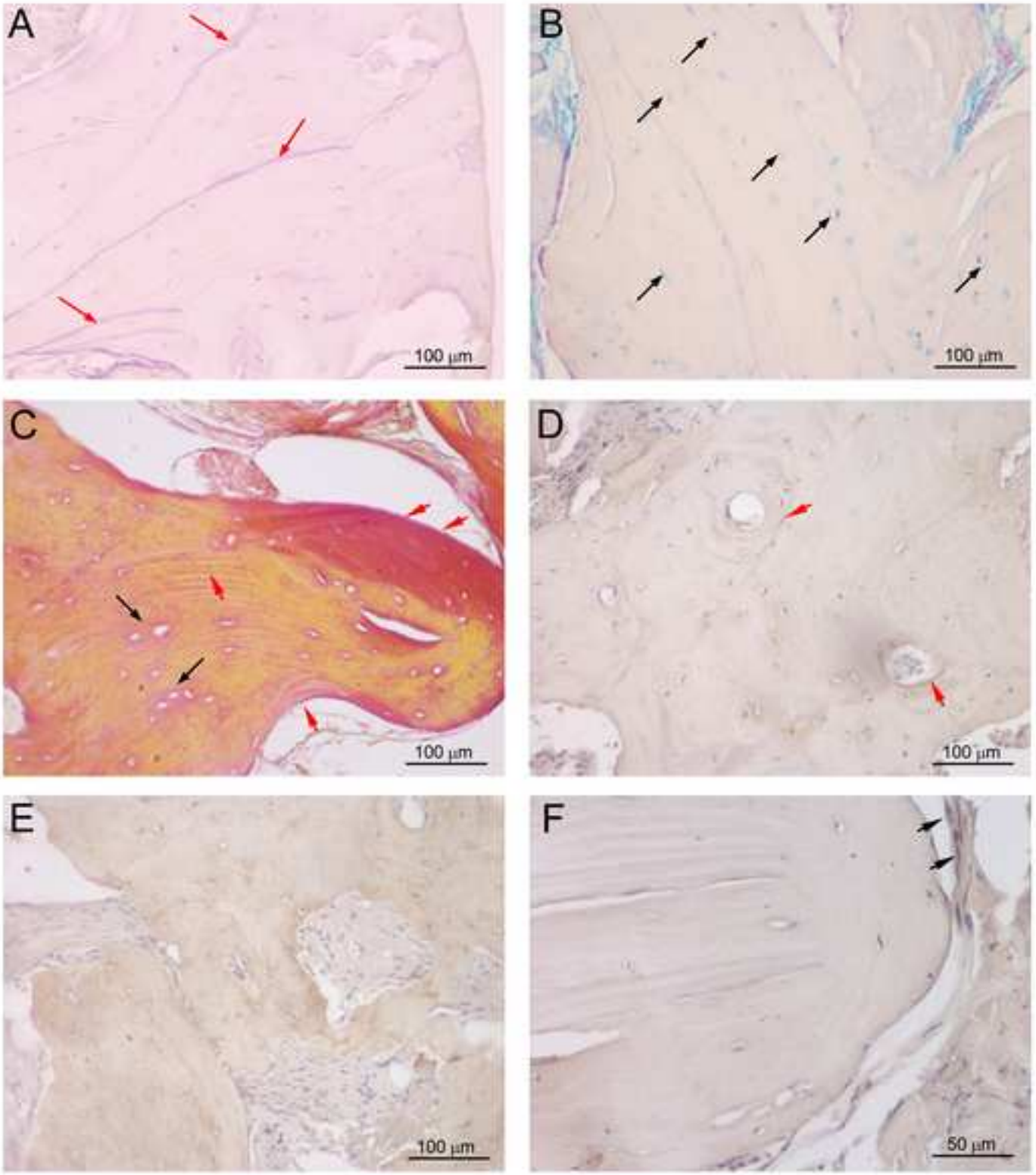

Figure 6

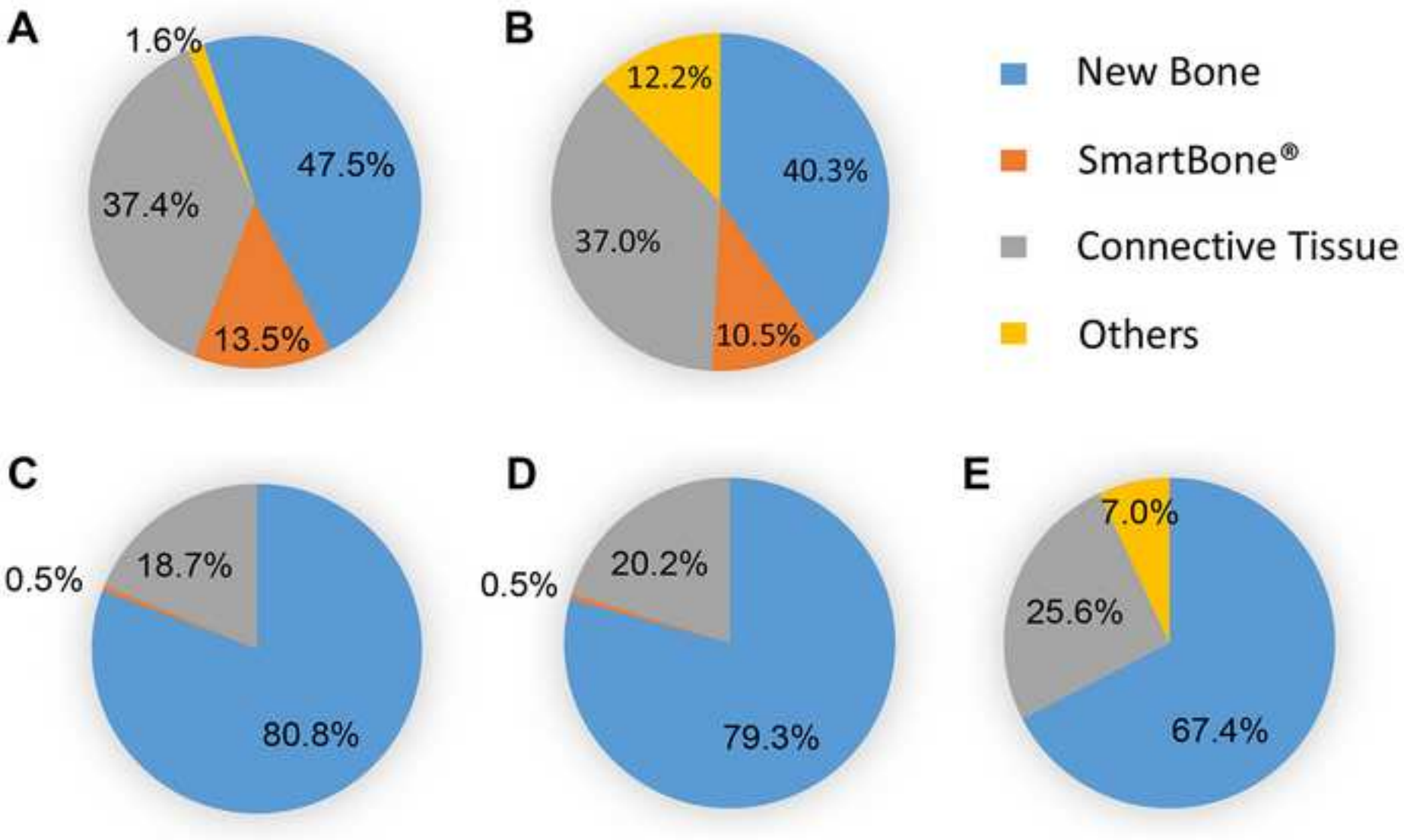
A
1.6%
47.5%
37.4%
13.5%
B
12.2%
40.3%
37.0%
10.5%
New Bone
SmartBone®
Connective Tissue
Others
C
0.5%
18.7%
80.8%
D
0.5%
20.2%
79.3%
E
7.0%
25.6%
67.4%

Supplementary Material

Click here to download Supplementary Material: Supplementary.pdf

*Graphical Abstract (for review)